IL NUOVO CIMENTO Vol. 34 C, N. 6 Novembre-Dicembre 2011
DOI 10.1393/ncc/i2011-11073-x

Colloquia: IFAE 2011

Updates on the most recent results in dual readout calorimetry

M. Cascella on behalf of the DREAM Collaboration
Università and INFN, Sezione di Pisa - Pisa, Italy

(ricevuto il 29 Luglio 2011; pubblicato online il 6 Dicembre 2011)

Summary. — The Dual REAdout Method (DREAM) consists in comparing the scintillation and Cherenkov light generated in the shower development process. By comparing the two, the electromagnetic fraction of the hadronic shower can be measured event-by-event, to eliminate the effects of fluctuations in this fraction. In this paper the DREAM fiber calorimeter and its successor, the newDREAM prototype that is currently under construction, will be described. We will also report on the efforts to study the Cherenkov component of the output of high-Z crystals and to realize a dual-readout electromagnetic section that can achieve outstanding electromagnetic resolution whitout compromising the hadronic resolution.

PACS 29.40.Vj – Calorimeters.
PACS 06.20.fb – Standards and calibration.
PACS 29.40.Ka – Cherenkov detectors.
PACS 29.40.Mc – Scintillation detectors.

1. – Introduction

The DREAM Collaboration [1] has the goal of developing a calorimeter that approaches the theoretical resolution limit in hadronic energy measurements. The dual readout approach consists of measuring event-by-event both the scintillation and Cherenkov light signal and use them to estimate the magnitude of the electromagnetic component of the shower.

Scintillation light (S) is due to ionization while Cherenkov light (C) is produced by relativistic particles, *i.e.* almost exclusively by the electromagnetic component of the hadronic shower. The simultaneous measurement of both components results in a better resolution and linearity: the ratio of the two signals can be expressed as a function of the fraction of the shower energy transported by electromagnetic particles f_{em}:

$$\frac{C}{S} = \frac{f_{em} + \lambda_C(1 - f_{em})}{f_{em} + \lambda_S(1 - f_{em})}, \tag{1}$$

λ_C and λ_S are the h/e ratios for the material that produces, respectively, the Cherenkov and the scintillation signal. This equation can be inverted to determine the value of f_{em}.

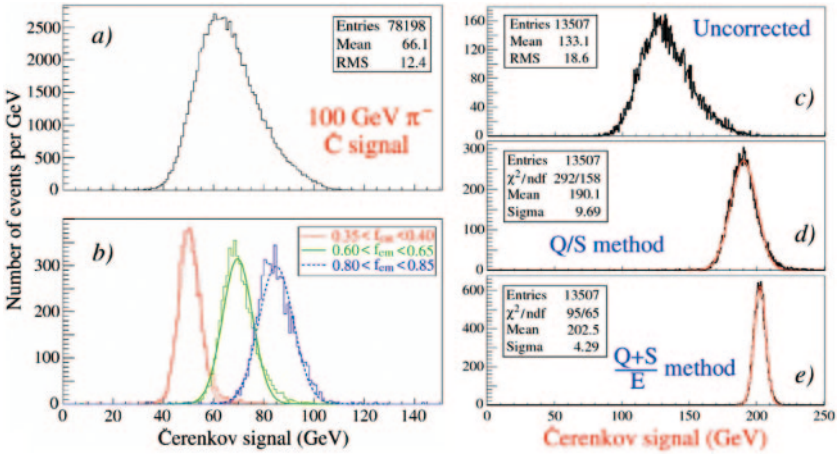

Fig. 1. – Cherenkov signal distribution for 100 GeV π^-(a) and distributions for three different bins of f_{em}(b). Signal distributions for high-multiplicity 200 GeV "jets" in the DREAM before (c) and after (d) C/S-based corrections. To eliminate the effects of lateral leakage that dominate the resolution in (d) energy constraints were imposed (e).

2. – The dual-readout method with fiber calorimeters

The dual readout method has first been tested with the DREAM prototype, a sampling calorimeter with copper as the absorber medium, and scintillating and clear fibers as the active medium. The Cherenkov light produced in the high-density clear fibers is read out separately. Figure 1 shows an example of the dual-readout approach: the Cherenkov signal for 100 GeV π^- is divided in 3 samples with different f_{em} each with a much smaller resolution. The many results obtained with the DREAM calorimeter have been presented in [1].

2˙1. *The newDREAM prototype module.* – The main factors that limit the DREAM calorimeter performance were identified in the low Cherenkov photoelectrons yield (that greatly contributes to the C resolution), the lateral and longitudinal leakage and the sampling fluctuations. For this reason a new generation of fiber modules using either copper or lead as the absorber material are being tested. The newDREAM modules has a sampling fraction of 5% (almost two times that of DREAM) aluminized clear fibers with a larger numerical aperture and the final assembled calorimeter will have 99% lateral containment. Finally we plan to sample the time structure of the signals with a DRS-IV–based acquisition to correct for light attenuation effects.

The Domino Ring Sampler chip. The DRS-IV chip [2] is the a multichannel sampler that offers both a very fast sampling and a wide buffer. The chip has 8+1 channels each with 1024 sampling capacitors on a single chip, a so-called "Domino wave" circuit generates a short pulse which opens analogue switches at the input of sampling cells of each channel. The Domino wave can be stopped by an external trigger, after which the sampling capacitors are read out and digitized by a commercial ADC.

The excellent characteristics of the DRS-IV chip has enabled us to sample with high resolution the time structure of the PMT signals.

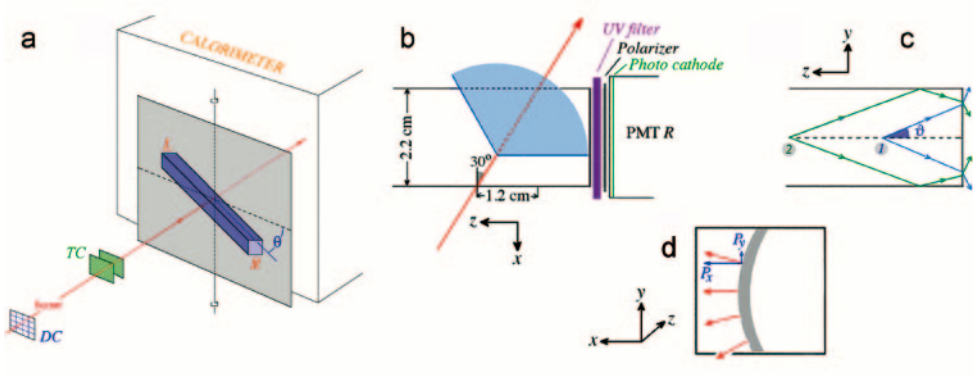

Fig. 2. – Experimental setup: placement of the crystals on the beam line (a). Development of the Cherenkov light cone in a crystal and placement of the UV and polarizing filters (b). Direction of the Cherenkov light polarization with respect to the light cone (c, d).

3. – Cherenkov - scintillation separation in crystals

High-Z crystals such as $PbWO_4$ (lead tungstate), BGO (bismuth germanate) and BSO (bismuth silicate) produce a significant amount of Cerenkov light (it contributes to up to 15% of the signal generated by high-energy particles traversing a $PbWO_4$ crystal [3]), which may be separated from the scintillation light by exploiting differences in time structure, directionality, spectral properties and polarization.

The experimental setup used in the crystal studies is detailed in fig. 2a which shows a schematic of the placement of the crystals on the beam line. Crystals are readout on both sides, usually with a different filter setup on each side.

3˙1. *Time structure.* – The Cherenkov light is a very fast signal while the scintillation signal is characterized by longer decay constants. This can be exploited using two gates to measure the Cherenkov and scintillation signal in the same channel as shown in fig. 3a. If the timing structure of the signal is available a template fitting technique can be used to obtain an even better result.

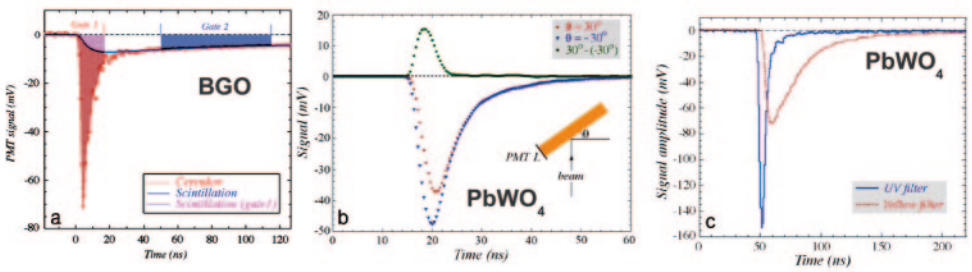

Fig. 3. – The time structure of a typical shower signal measured in the BGO electromagnetic calorimeter equipped with a UV filter (a), in a $PbWO_4$ crystal with no filters where the Cherenkov signal is estimated by taking the difference between the signal on the two sides (b) and in the same crystal readout with a UV filter on the $-30°$ side and a yellow filter on the other (c).

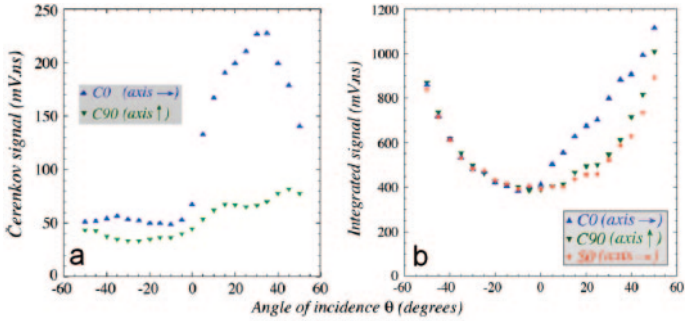

Fig. 4. – Average amplitude (a) and integral (b) of the signals of 180 GeV π^+ traversing a BSO crystal as a function of the angle θ. Results are given for the Cherenkov signals corrected for the path length, with the transmission axis of the polarization filter oriented in the horizontal plane (C0), the vertical plane (C90) and for the scintillation signals with the transmission axis in the horizontal plane (S0).

3˙2. *Direction.* – By placing the crystal at the Cherenkov angle with respect to the direction of the beam we can exploit the directionality of Cherenkov light collect most of it on one side (see fig. 2b). Figure 3b shows how the Cherenkov signal can be reconstructed as the difference of the light measured at the two ends of a $PbWO_4$ crystal.

3˙3. *Wavelength.* – Cherenkov light spans the UV and blue regions of the spectrum while scintillation light is mainly produced in the visible range. We take advance of this by using a yellow filter to only select scintillation light and a UV filter to readout Cherenkov light [5]. In this way, an excellent separation of the two components can be obtained as shown in fig. 3c.

An example of the spectral and directional separation can be seen in fig. 5c showing the angular dependence of the ratio of the Cherenkov and scintillation signals (selected using UV and yellow filters) in BSO and BGO crystals.

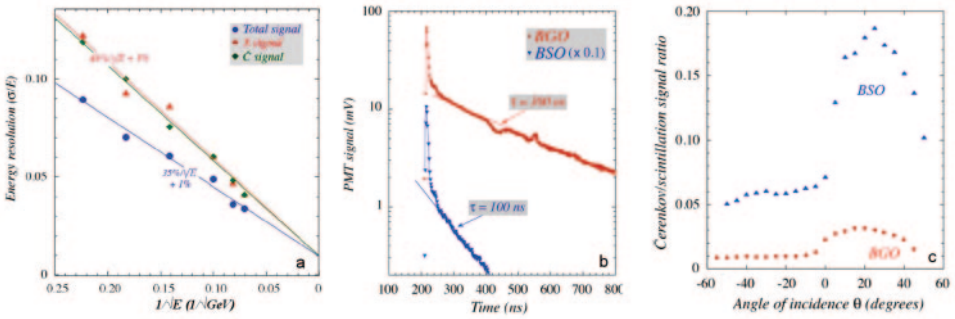

Fig. 5. – The energy resolution of a BGO DREAM calorimeter as a function of energy plotted separately for the scintillation and Cherenkov components and for the total signal (a). Comparison of a BSO and a BGO crystal: average profile of the light output (b) and Cherenkov/Scintillation ratio as a function of the angle (c).

3˙4. *Polarization*. – The characteristic polarization of Cherenkov light (see fig. 2c and 2d) has been exploited to separate the two light components [6].

Figure 4a shows better how large the effect of the polarization filter is. The Cherenkov component is reduced by a factor of about 3.5 as a result of the rotation of the transmission axis of the polarization filter from the horizontal to the vertical plane. The same effect is visible, even if less pronounced, in the integrated signal (fig. 4b).

4. – Toward a dual-readout homogeneous DREAM calorimeter

A full-size dual readout electromagnetic calorimeter made of 100 BGO crystals recovered from the L3 experiment was tested using the time structure method to separate the Cherenkov from the scintillation signal [7]. Since the characteristics of the setup limited the achievable resolution (fig. 5c shows the electromagnetic resolution) the matrix has been equipped with a new array of PMT with and improved optical coupling and is currently under test.

A number of BSO crystals have been also characterized and compared with BGO crystals. BSO represent a viable alternative to BGO crystals and present a number of advantages namely faster scintillation (see fig. 5b) and a much higher C/S ratio (fig. 5c) around the Cherenkov angle [8].

After a careful work of characterization of a series of doped $PbWO_4$ crystals [9] a small matrix of 7 crystals read on the two sides with UV and yellow filters has been built and is undergoing testing as an alternative for a dual-readout electromagnetic stage.

5. – Final remarks

The dual readout of Cherenkov and scintillation light make it possible to estimate event-by-event the f_{em} of the hadronic shower reducing the effect of its fluctuations on the resolution. This technique has been extensively tested on both sampling and homogeneous calorimeters. The DREAM Collaboration keeps exploring and addressing all the factors that limit hadronic calorimetry resolution.

REFERENCES

[1] Akchurin N. *et al.*, *Nucl. Instrum Methods A*, **533** (2004) 305; **536** (2005) 29; **537** (2005) 537; **548** (2005) 336; **550** (2005) 185.
[2] Ritt S. *et al.*, *Nucl. Instrum. Methods A*, **623** (2010) 486.
[3] Akchurin N. *et al.*, *Nucl. Instrum. Methods A*, **582** (2007) 474.
[4] Nikl M. *et al.*, *J. Appl. Phys.*, **91** (2002) 2792.
[5] Akchurin N. *et al.*, *Nucl. Instrum. Methods A*, **595** (2008) 359.
[6] Akchurin N. *et al.*, *Nucl. Instrum. Methods A*, **638** (2011) 47.
[7] Akchurin N. *et al.*, *Nucl. Instrum. Methods A*, **610** (2009) 488.
[8] Akchurin N. *et al.*, *Nucl. Instrum. Methods A*, **640** (2011) 91.
[9] Akchurin N. *et al.*, *Nucl. Instrum. Methods A*, **621** (2010) 212.